The transcription factors ZEB2 and T-bet cooperate to program cytotoxic T cell terminal differentiation in response to LCMV viral infection

Claudia X. Dominguez,[1]* Robert A. Amezquita,[1,4]* Tianxia Guan,[1,4]* Heather D. Marshall,[1] Nikhil S. Joshi,[1] Steven H. Kleinstein,[1,2,3] and Susan M. Kaech[1,4]

[1]Department of Immunobiology, [2]Interdepartmental Program in Computational Biology and Bioinformatics, and [3]Department of Pathology, Yale University School of Medicine, New Haven, CT 06520
[4]Howard Hughes Medical Institute, Chevy Chase, MD 20815

<div style="margin-left: 2em; font-style: italic; display: block;">The Journal of Experimental Medicine</div>

The transcription factor T-bet is critical for cytotoxic T lymphocyte (CTL) differentiation, but it is unclear how it operates in a graded manner in the formation of both terminal effector and memory precursor cells during viral infection. We find that, at high concentrations, T-bet induced expression of *Zeb2* mRNA, which then triggered CTLs to adopt terminally differentiated states. ZEB2 and T-bet cooperate to switch on a terminal CTL differentiation program, while simultaneously repressing genes necessary for central memory CTL development. Chromatin immunoprecipitation sequencing showed that a large proportion of these genes were bound by T-bet, and this binding was altered by ZEB2 deficiency. Furthermore, T-bet overexpression could not fully bypass ZEB2 function. Thus, the coordinated actions of T-bet and ZEB2 outline a novel genetic pathway that forces commitment of CTLs to terminal differentiation, thereby restricting their memory cell potential.

CD8^{+} T cells are a critical component of cell-mediated immunity against intracellular pathogens, such as viruses, and can provide long-term protection from reinfection for decades after the initial infection is cleared (Ahmed and Gray, 1996; Jameson and Masopust, 2009). Despite the importance of cytotoxic T lymphocyte (CTL) immunity in controlling viral infections, a successful T cell–based vaccine has yet to be developed. Many intracellular pathogens for which we still lack effective vaccines, such as HIV, involve pathogens that can escape neutralizing antibody; a T cell–based vaccine strategy may improve protection from such pathogens. Harnessing this potential requires greater immunological insight into how T cell memory forms after infection and vaccination.

Our understanding of effector and memory T cell development has advanced considerably over the past decade. In response to acute infections, CD8^{+} T cells expand into a heterogeneous population of effector cells that can be phenotypically, functionally, and anatomically distinguished. Importantly, the long-term fates of the effector cells also differ after infection in that the majority of cells (∼90–95%) die and a minority persist to give rise to longer-lived memory T cells (Ahmed and Gray, 1996; Jameson and Masopust, 2009; Kaech and Cui, 2012). Often, increased IL-7 receptor

α (IL-7R) expression on effector cells identifies those with a higher potential to persist and seed diverse populations of central memory (T_{CM}), effector memory (T_{EM}), and resident memory (T_{RM}) T cells (Sallusto et al., 1999; Schluns et al., 2000; Kaech et al., 2003; Huster et al., 2004; Joshi et al., 2007; Jameson and Masopust, 2009; Kaech and Cui, 2012; Mackay et al., 2013). These antigen-specific IL-7R^{+} CD8^{+} T cells, commonly referred to as memory precursor (MP) cells, are endowed with longevity and the ability to self-renew and regenerate new clonal bursts of effector cells (i.e., they are multipotent). Conversely, terminally differentiated effector (TE) cells, often identified by killer-cell lectin-like receptor G1 (KLRG1) expression, are potent killers and IFN-γ secretors that have decreased longevity, proliferative potential, and restricted plasticity (Voehringer et al., 2001; Thimme et al., 2005; Joshi et al., 2007, 2011; Olson et al., 2013). This divergence in long-term fates raises the questions: How is the process of terminal differentiation programmed and how is plasticity maintained in CTLs as they differentiate during infection?

Gene expression profiling experiments have identified unique transcriptional signatures for MP cells (KLRG1^{lo} IL-7-R[hi]) and TE cells (KLRG1^{hi} IL7R^{lo}; Joshi et al., 2007; Rutishauser et al., 2009; Best et al., 2013; Arsenio et al., 2014). Further, T-bet (encoded by *Tbx21*), B lymphocyte-induced maturation protein-1 (Blimp-1, encoded

---

The Rockefeller University Press $30.00
J. Exp. Med. 2015 Vol. 212 No. 12   2041–2056
www.jem.org/cgi/doi/10.1084/jem.20150186

2041

by *Prdm1*), inhibitor of DNA binding 2 (*Id2*), and signal transducer and activator of transcription 4 (*Stat4*) have been identified as critical drivers of TE cell differentiation (Joshi et al., 2007; Kallies et al., 2009; Rutishauser et al., 2009; Yang et al., 2011; Mollo et al., 2013; Shin et al., 2013). Conversely, expression of eomesodermin (Eomes), B cell lymphoma-6 (*Bcl6*), T cell factor-7 (*Tcf7*), *Id3*, forkhead box O 1 (*Foxo1*), and *Stat3* promote development of memory CD8$^+$ T cells and their progenitors (Ichii et al., 2002, 2004; Jeannet et al., 2010; Zhou et al., 2010; Cui et al., 2011; Yang et al., 2011; Hess Michelini et al., 2013; Kim et al., 2013; Tejera et al., 2013). However, little is known about how these transcription factors interact or affect each other's expression or function to develop distinct subsets of CTLs with diverse cell fates. Small differences in the amounts of some of these transcriptional regulators can have profound effects on CTL fate. For example, T-bet operates in a graded manner in effector CTLs, with moderate levels permitting memory cell fates but relatively higher levels promoting terminal differentiation (Joshi et al., 2007). Mechanistically, how modest differences in T-bet expression translate into distinct changes in gene expression, function, and specification of long-term fates in CTLs is not clear.

This study identifies a novel role for the transcription factor ZEB2 as one such translator of high T-bet expression. We find *Zeb2* mRNA is highly expressed in terminally differentiated CTLs, in agreement with results from studies profiling gene expression in CTLs (Rutishauser and Kaech, 2010; Wirth et al., 2010; Best et al., 2013; Arsenio et al., 2014), and that this occurs in a T-bet–dependent manner. Deletion of ZEB2 reveals that it is necessary for normal TE cell expansion and transcriptional programming. Whole-transcriptome RNA sequencing (RNA-seq) analysis of WT, *Tbx21*$^{-/-}$, and *Zeb2*$^{-/-}$ CTLs identified a set of genes whose expression was dependent on both T-bet and ZEB2, and suggested that they cooperate to promote TE genes while repressing MP genes. ZEB2 deficiency also affected T-bet binding to TE and MP cell signature loci, resulting in enhanced T-bet binding at several MP cell signature gene loci, suggesting T-bet alone cannot repress these genes. Motif enrichment analysis revealed that many of these MP loci contained putative ZEB2-binding sites, suggesting coordinated regulation of T-bet binding by ZEB2. Furthermore, overexpression of T-bet could not fully restore TE differentiation in ZEB2-deficient CTLs, particularly the repression of several MP cell signature genes, suggesting ZEB2 is necessary for the repression of this genetic program along with T-bet. Moreover, *Zeb2* was necessary in TE cells to promote maximal expression of TE cell signature genes in conjunction with T-bet. Thus, we have identified ZEB2 as a developmental trigger, induced by higher amounts of T-bet, that works in conjunction with T-bet to switch off MP- and switch on TE-signature genes; ultimately, this process drives terminal CTL differentiation by restricting effector cell plasticity and memory cell potential.

RESULTS

Zeb2 is expressed in KLRG1^{hi} CD8$^+$ T cells in a T-bet–dependent manner

To examine the *Zeb2* mRNA expression pattern in virus-specific CTLs during lymphocytic choriomeningitis virus (LCMV) infection, B6 mice were infected with the Armstrong strain of LCMV (LCMV-Arm), which causes an acute viral infection. Naive (CD44^{lo}) CD8$^+$ T cells were sorted from uninfected mice and MHC class I tetramer$^+$ LCMV-specific CTLs were purified from infected mice at 6, 8, and >60 d postinfection (d.p.i.). The virus-specific CTLs were further subdivided to compare *Zeb2* mRNA levels between more differentiated (KLRG1^{hi}) and less differentiated (KLRG1^{lo}) CD8$^+$ T cells (Fig. 1 a). *Zeb2* mRNA was not detectable in naive CD8$^+$ T cells, but was induced in effector and memory CD8$^+$ T cells, most dramatically in the KLRG1^{hi} cells (Fig. 1 a). *Tbx21* mRNA transcript expression showed an expression pattern similar to *Zeb2* mRNA across both subsets and over time (Fig. 1 b), demonstrating the direct correlation of *Zeb2* and *Tbx21* expression in CTL subsets. In our hands, commercially available antibodies could not detect murine ZEB2 protein in CTLs, and lentiviral overexpression of a flag-tagged ZEB2 proved toxic in activated CD8$^+$ T cells (unpublished data); thus, we were unable to measure or isolate ZEB2 protein by conventional methods in this study.

As T-bet controls the development of TE cells in a graded manner (Joshi et al., 2007, 2011), we next evaluated whether the induction of *Zeb2* mRNA in effector CD8$^+$ T cells was dependent on the amount of T-bet expressed by the CTLs. To do this, we generated P14 chimeric mice by transferring small numbers (∼5,000) of *Tbx21*$^{+/+}$ WT), *Tbx21*$^{+/-}$, or *Tbx21*$^{-/-}$ P14 CD8$^+$ T cells, specific for the D^{b}GP$_{33-41}$ epitope of LCMV, into B6 recipient mice that were subsequently infected with LCMV-Arm. This transfer system ensured the analysis of only CD8$^+$ T cell–intrinsic effects of T-bet deficiency on *Zeb2* mRNA expression. Similar to the polyclonal CTLs, *Zeb2* mRNA was most abundant in the KLRG1^{hi} P14 CTLs, particularly the KLRG1^{hi} IL-7R^{lo} subset (Fig. 1 c). Although fewer KLRG1^{hi} cells formed in *Tbx21*$^{+/-}$ and *Tbx21*$^{-/-}$ CTLs, a sufficient number of KLRG1^{hi} IL-7R^{lo} effector cells could be obtained for qPCR analysis, and this revealed a direct correlation between T-bet copy number and *Zeb2* mRNA levels. That is, KLRG1^{hi} IL-7R^{lo} cells lacking one copy of T-bet (*Tbx21*$^{+/-}$) expressed 30–60% less *Zeb2* mRNA than their WT counterparts, and those lacking both copies of T-bet (*Tbx21*$^{-/-}$) expressed 90% less (Fig. 1 d). These data suggested that increased amounts of T-bet are needed for maximal *Zeb2* mRNA expression in CTLs.

To determine whether T-bet directly bound to the *Zeb2* locus, chromatin immunoprecipitation-sequencing (ChIP-seq) was performed on virus-specific CD8$^+$ T cells with anti–T-bet antibodies. This identified predominant regions of T-bet binding at the *Zeb2* transcriptional start site (TSS) and 3 kb upstream of the TSS (Fig. 1 e). Both of these sites contained histone H3K27 acetylation, suggesting the locus
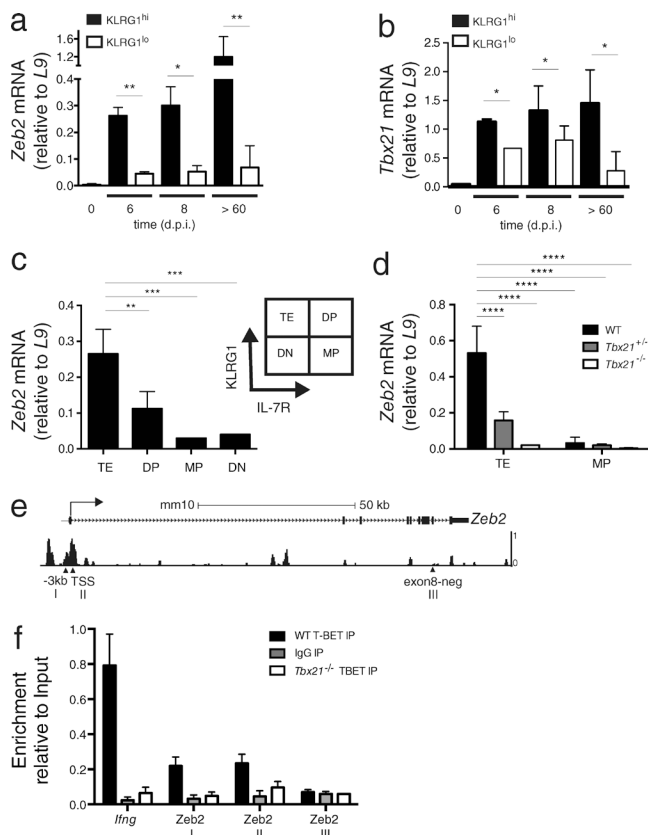
Figure 1. **ZEB2 is expressed in terminally differentiated effector CTLs in a T–bet–dependent manner.** (a and b) *Zeb2* mRNA (a) or *Tbx21* mRNA (b) was measured in purified CD44^{lo} CD62L^{hi} naive CD8$^+$ T cells (day 0) or KLRG1^{hi} (black bars) or KLRG1^{lo} (white bars) LCMV-specific CD8$^+$ T cells from 6, 8, or >60 d.p.i. using qRT-PCR. LCMV-specific CD8$^+$ T cells were isolated based on staining for D^{b}GP$_{33-41}$-tetramer. (c) Effector P14 CD8$^+$ T cells isolated 8 d.p.i. were purified based on KLRG1^{hi} IL-7R^{lo} (TE), KLRG1^{hi} IL-7R^{hi} (double positive, DP), KLRG1^{lo} IL-7R^{hi} (MP), or KLRG1^{lo} IL-7R^{lo} (double negative, DN) expression and the amount of *Zeb2* mRNA was measured in the indicated subsets using qRT-PCR. (d) *Zeb2* mRNA levels were compared between sorted WT, *Tbx21$^{+/-}$*, and *Tbx21$^{-/-}$* TE (KLRG1^{hi} IL-7R^{lo}) or MP (KLRG1^{lo} IL-7R^{hi}) P14 CTLs 8 d.p.i. (e) T-bet ChIP-seq was performed on effector P14 CD8$^+$ T cells isolated 8 d.p.i. and stimulated in brief with IL-12. T-bet binding was visualized using the UCSC Genome Browser. Outline of the murine *Zeb2* locus with exons (black boxes), the transcriptional start site (TSS, probe II), an additional T-bet binding site (−3 kb, probe I), and an internal negative control site (exon8-neg, probe III) noted. (f) Bar graph shows the amount of T-bet bound to regions I and II in the *Zeb2* locus in WT (black bars) or *Tbx21$^{-/-}$* (white bars) effector P14 CTLs from 8 d.p.i. based on ChIP using anti–T-bet or isotype IgG control (gray bars), followed by qRT-PCR. T-bet binding to the *IFN*γ promoter or *Zeb2* exon8 are shown as positive and negative controls, respectively (Cho et al., 2003). Data shown in a–d and f are representative of three to five experiments (*n* = 4–5 mice/group/independent experiment); panel e displays data from a single sequencing run. Bars represent mean expression ± SEM. *, P < 0.05; **, P < 0.01; ***, P < 0.001.

was transcriptionally active (unpublished data). Additionally, these binding sites were validated by ChIP-qPCR in WT and *Tbx21$^{-/-}$* virus–specific CD8$^+$ T cells (the *Ifng* promoter and a third region in exon 8 of *Zeb2* served as positive and negative controls, respectively; Fig. 1 f). These data show that T-bet binds directly to the *Zeb2* locus, providing stronger evidence that T-bet acts as a direct transcriptional activator of ZEB2 in virus–specific CTLs.

Effector and memory cell development in ZEB2–deficient CD8$^+$ T cells

To investigate the function of ZEB2 in CD8$^+$ effector T cell differentiation, *Zeb2* was deleted from activated CD8$^+$ T cells by crossing mice with floxed *Zeb2* alleles (*Zeb2$^{flox/flox}$*; Higashi et al., 2002) to mice expressing Cre recombinase under control of the Granzyme B promoter (*GzmB*-cre; Jacob and Baltimore, 1999). In this conditional knock-out system, the *Zeb2* locus remains intact until a naive CD8$^+$ T cell is activated and expresses *GzmB* and therefore also *GzmB-cre*. For simplicity, the *Zeb2$^{flox/flox}$*; *GzmB-cre$^+$* mice will be referred to as *Zeb2$^{-/-}$* mice and *Zeb2$^{flox/flox}$*; *GzmB-cre$^-$* or *Zeb$^{+/+}$*; *GzmB-cre$^+$* littermate controls will be referred to as WT mice. It was important to use a conditional knock-out strategy because *Zeb2$^{-/-}$* mice show embryonic lethality and *Zeb2* is expressed in many cell types, including hematopoietic stem cells, NK cells, monocytes, and mast cells (Tylzanowski et al., 2003; van Grunsven et al., 2006; Goossens et al., 2011; Barbu et al., 2012; Best et al., 2013). *Zeb2* was efficiently deleted in ∼85–90% of the polyclonal CD44^{hi} CD8$^+$ T cells using this system (unpublished data).

ZEB2-deficient CD8$^+$ T cells underwent clonal expansion and CTL differentiation during LCMV infection, but the numbers of *Zeb2$^{-/-}$* tetramer-specific CTLs was reduced by ∼50% at 8 d.p.i. Furthermore, the *Zeb2$^{-/-}$* effector CTLs displayed accelerated rates of contraction, although by 60 d.p.i. similar numbers of *Zeb2$^{-/-}$* and WT memory cells persisted (Fig. 2 a). The ZEB2-deficient CTLs appeared to have no gross defects in cytotoxicity based on in vivo CTL-killing assays (Fig. 2 b). Similarly, the ability of *Zeb2$^{-/-}$* and WT CTLs to produce IFN-γ and TNF was comparable (Fig. 2 c, left). However, CTLs lacking *Zeb2* produced more IL-2 than WT cells (Fig. 2 c, right). These results indicated that ZEB2 promoted effector cell clonal expansion and survival during acute viral infection, but was dispensable for cytotoxicity as well as IFN-γ and TNF production. However, ZEB2 appeared to restrict polyfunctionality by suppressing IL-2 production in CTLs.

Because increased IL-2 production is a property of T$_{CM}$ cells (Sallusto et al., 1999; Wherry et al., 2003b), we postulated that ZEB2 might repress the development of T$_{CM}$ cells. Indeed, analysis of memory P14 *Zeb2$^{-/-}$* CTLs showed an accumulation of memory T cells with T$_{CM}$ phenotypes, such as decreased KLRG1 and increased L-selectin (CD62L), B
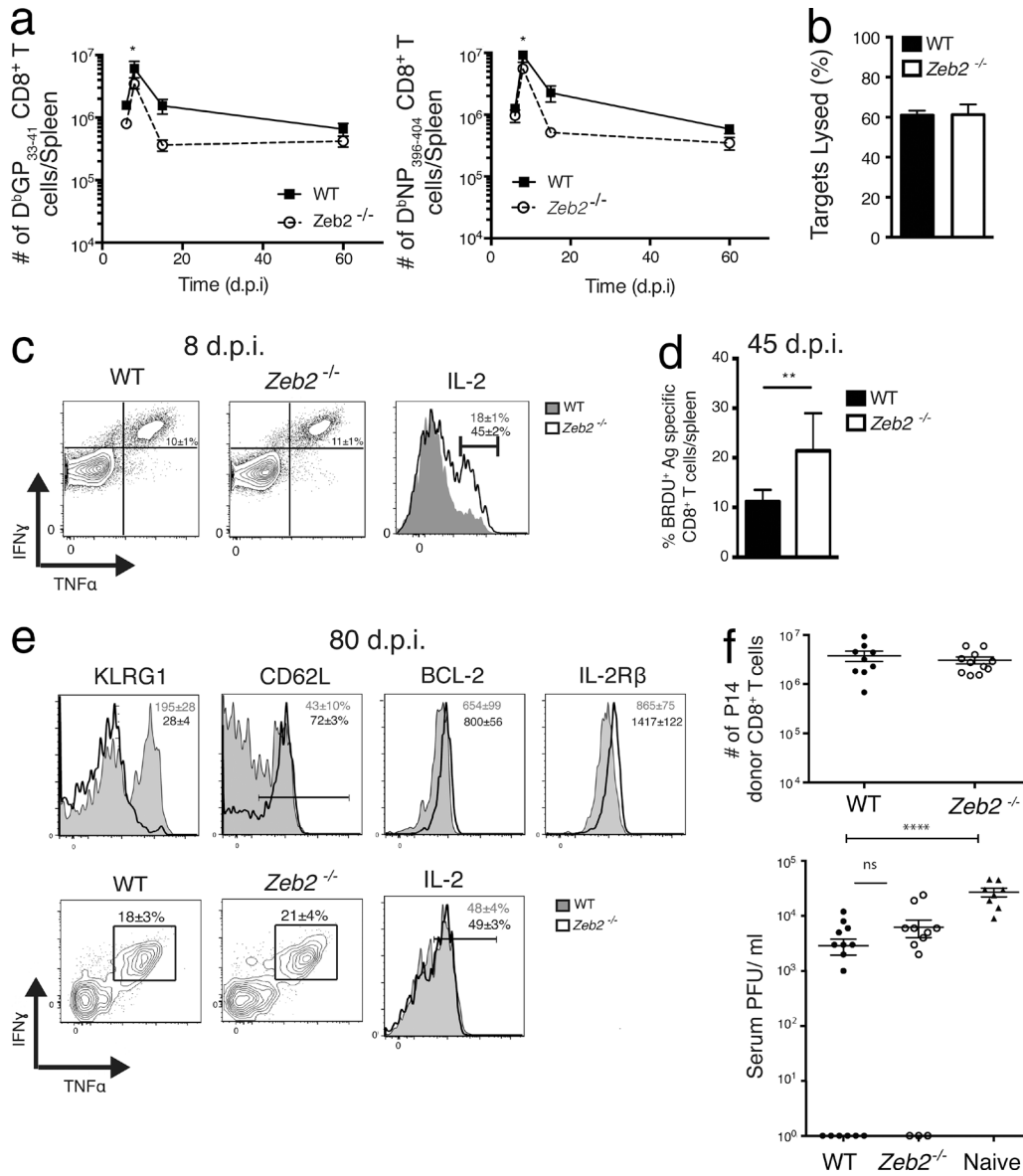
Figure 2. **ZEB2–deficient CD8+ T cells acquire CTL functions during LCMV infection.** (a) WT (filled square) and $Zeb2^{-/-}$ (open circle) mice were infected with LCMV and splenic D^bGP_{33-41} and $D^bNP_{396-404}$ tetramer+ CTLs were quantitated at 6, 8, 15, and 60 d.p.i. Data pooled for each time point are from two (day 6) or >3 (day 8–60) independent experiments containing three to five mice per group. (b) in vivo cytotoxicity assays using CFSE-labeled GP_{33-41} peptide-coated splenocytes as targets were performed in LCMV-infected WT or $Zeb2^{-/-}$ mice at 8 d.p.i. Data are pooled from two independent experiments (n = 3–4 mice/group). (c) WT and $Zeb2^{-/-}$ CTLs from 8 d.p.i. were analyzed for IFNγ and TNF (left contour plots) or IL-2 (right histogram plots) expression using intracellular cytokine staining after a 5-h GP_{33-41} peptide stimulation. Note, IL-2–producing cells were gated on IFNγ+ TNF+ CTLs. Data are representative of >6 independent experiments (n = 4–5 mice/group). (d) To measure rates of homeostatic turnover in memory CD8+ T cells, mice infected with LCMV-Arm 35 d before were administered BrdU in their drinking water for 10 d, and the frequency of BrdU+ D^bGP_{33-41} and $D^bNP_{396-404}$ tetramer+ CTLs in the spleen was determined by intracellular staining and flow cytometry at 45 d.p.i. Data are pooled from two independent experiments containing n = 3–5 mice/group. (e) P14 chimeric mice were infected with LCMV-Arm and sacrificed at 80 d.p.i. and analyzed for expression of KLRG1, CD62L, Bcl-2, and IL-2Rβ (top) as well as cytokine production in response to peptide restimulation (bottom) Histograms show percentage or MFI of markers as indicated. IL-2 expression plot is gated on IFN-γ and TNF double-producing cells. Data are representative of two independent experiments containing n = 5 mice/group. Bars represent mean expression ± SEM. (f) For rechallenge experiments, 60,000 memory WT (black circles) or $Zeb2^{-/-}$ (open circles) P14 CD8+ T cells (from 60+ d.p.i.) were transferred into naive mice that were then infected with clone 13 LCMV. 6 d later, the number of donor P14 CTLs in the spleen (top) and viral titers in the serum (bottom) were measured. Data are representative of three independent experiments containing n = 3–5 mice/group. Bars represent mean expression ± SEM. *, $P < 0.05$; **, $P < 0.01$; ****, $P < 0.0001$.

cell lymphoma 2 (BCL-2), and interleukin receptor 2 β (IL-2Rβ) expression (Fig. 2 e). The phenotype of *Zeb2*-deficient memory CD8$^+$ T cells suggested the rate of T$_{CM}$ formation after LCMV infection was accelerated in these mice. Functionally, there were no gross defects in the ability of ZEB2-deficient memory cells to produce cytokines or homeostatically turn over (Fig. 2, d and e). Transferred P14 *Zeb2*$^{-/-}$ memory CTLs retained the ability to protect recipient animals upon challenge with the chronic strain of LCMV clone13, expanding and controlling serum viremia similar to WT memory cells (Fig. 2 f). These data indicated that memory CD8$^+$ T cell homeostasis and recall responses were largely unperturbed by *Zeb2* deficiency.

ZEB2 represses MP gene expression in TE cells

Examination of virus-specific *Zeb2*$^{-/-}$ CTL subsets by flow cytometry revealed a significant reduction in the frequency of KLRG1^{hi} IL-7R^{lo} TE cells and, consequently, an increase in the frequency of all other populations (Fig. 3 a). However, when cell numbers were calculated, there was only a significant reduction in the number of TE cells, without a corresponding increase in any other population (Fig. 3 a). Furthermore, the TE-like cells that were present in the *Zeb2*$^{-/-}$ effector population actually expressed less surface KLRG1 (based on mean fluorescence intensity [MFI]) and *Gzma* mRNA (based on RT-PCR) and had ectopic expression of several MP cell–associated genes, such as CD27 (encoded by *Tnfrsf7*) and the chemokine receptor C-X-C receptor 3 (CXCR3; Fig. 3 b). Therefore, we next analyzed the transcription factors involved in MP and TE cell fate determination, which revealed that the *Zeb2*$^{-/-}$ TE-like cells contained substantially lower amounts of T-bet protein and *Prdm1* (Blimp-1) mRNA, two transcription factors necessary for TE cell development (Joshi et al., 2007; Kallies et al., 2009; Rutishauser et al., 2009; Shin et al., 2013), and conversely, increased amounts of TCF7, Eomes, and BCL6 protein, as well as *Klf4* and *Id3* mRNA, five transcription factors important for memory CD8 T cell development (Ichii et al., 2002, 2004; Kallies et al., 2009; Jeannet et al., 2010; Zhou et al., 2010; Cui et al., 2011; Shin et al., 2013; Fig. 3 c). In contrast, the expression of such pro–memory genes was not affected by *Zeb2* deficiency in the MP-like cells (Fig. 3, b and c).

ZEB2 and T–bet regulate an overlapping set of genes to promote TE cell transcriptional programming

Comparison of *Tbx21*$^{-/-}$ and *Zeb2*$^{-/-}$ CTLs revealed a high degree of phenotypic similarity (Fig. 4, a and b). Although substantially fewer KLRG1$^+$ cells formed in the absence of T-bet, de-repression of CD27, CXCR3, and Eomes was observed in these cells, similar to the *Zeb2*$^{-/-}$ TE cells (Fig. 4 b). Overall, this suggested that ZEB2 and T-bet may perform similar roles in TE cell differentiation. To investigate this in greater detail and to identify potential gene targets, we evaluated the genome-wide transcriptional profiles of *Tbx21*$^{-/-}$ and *Zeb2*$^{-/-}$ CTLs using RNA-seq (Fig. 4, c–f).

First, we defined MP and TE gene expression signatures by identifying genes differentially expressed between MP and TE cells at 8 d.p.i. (≥1.5 fold change with a false discovery rate [FDR] ≤ 0.1). We identified 1,458 genes that met these criteria, of which 777 were up-regulated in MP relative to TE cells, whereas conversely 687 genes were up-regulated in TE relative to MP cells. Next, we examined how the expression of the MP and TE cell signature genes was affected by T-bet or ZEB2 deficiency. We designated genes that were differentially expressed (≥1.5 fold change with a FDR ≤ 0.1) between the *Tbx21*$^{-/-}$ and WT CTLs or *Zeb2*$^{-/-}$ and WT CTLs as being T-bet or ZEB2 dependent, respectively (Fig. 4, e and f, red and blue gene sets). We referred to the set of genes differentially expressed in common between both knock-outs versus WT CTLs as the codependent gene set (Fig. 4, e and f, purple gene sets). These analyses showed that within both knock-out CTL populations there was a marked increase in the expression of many MP-signature genes and decrease in the expression of several TE-signature genes, with T-bet affecting a larger portion of these genes (Fig. 4 e). Importantly, supporting the notion that T-bet and ZEB2 cooperate to regulate CTL differentiation, a significant portion of TE and MP genes were codependent on both ZEB2 and T-bet function (Fig. 4, e and f, see purple codependent gene set).

To further analyze how T-bet and ZEB2 regulated the MP and TE cell signatures, we compared the differentially expressed genes in the knock-out CTLs to the MP- and TE-signature genes using volcano plots (Fig. 4 f). This clearly showed that genes up-regulated in *Tbx21*$^{-/-}$ or *Zeb2*$^{-/-}$ CTLs relative to their WT counterparts were preferentially enriched with MP-signature genes and conversely, those genes down-regulated were preferentially enriched with TE-signature genes. This pattern became even more apparent within the T-bet and ZEB2 codependent set of genes whose expression is altered in both *Zeb2*$^{-/-}$ and *Tbx21*$^{-/-}$ CTLs. Because the *Tbx21*$^{-/-}$ or *Zeb2*$^{-/-}$ CTL populations are comprised of different percentages of TE- and MP-like CTLs, we isolated the subsets of KLRG1^{hi} IL-7R^{lo} and KLRG1^{lo} IL-7R^{hi} effector cells from WT and *Zeb2*$^{-/-}$ CTLs to directly compare the MP- and TE-gene signatures within each cell subset by microarray analysis (Fig. 3 d). This analysis verified that *Zeb2* was required specifically in the KLRG1^{hi} IL-7R^{lo} cells for significant repression (* = FDR < 0.01) of several additional MP-signature genes, such as *Socs3*, *Il7r*, *Pou6f1*, *Ctla4*, *Tcf7*, and *Ltb*, and promotion of several TE-signature genes, such as *Klra3*, *Klre1*, and *Itgam*, in addition to the others shown in Fig. 3 (b and c). In contrast, none of the MP- or TE-signature genes were significantly differentially expressed in *Zeb2*$^{-/-}$ MP cells compared with WT MP cells, in line with the low amounts of *Zeb2* mRNA in this cell subset (Fig. 3 d).

The genes affected by T-bet and ZEB2 deficiency can be assigned to various functional categories involved in CTL differentiation, including transcriptional regulation, T cell mi-
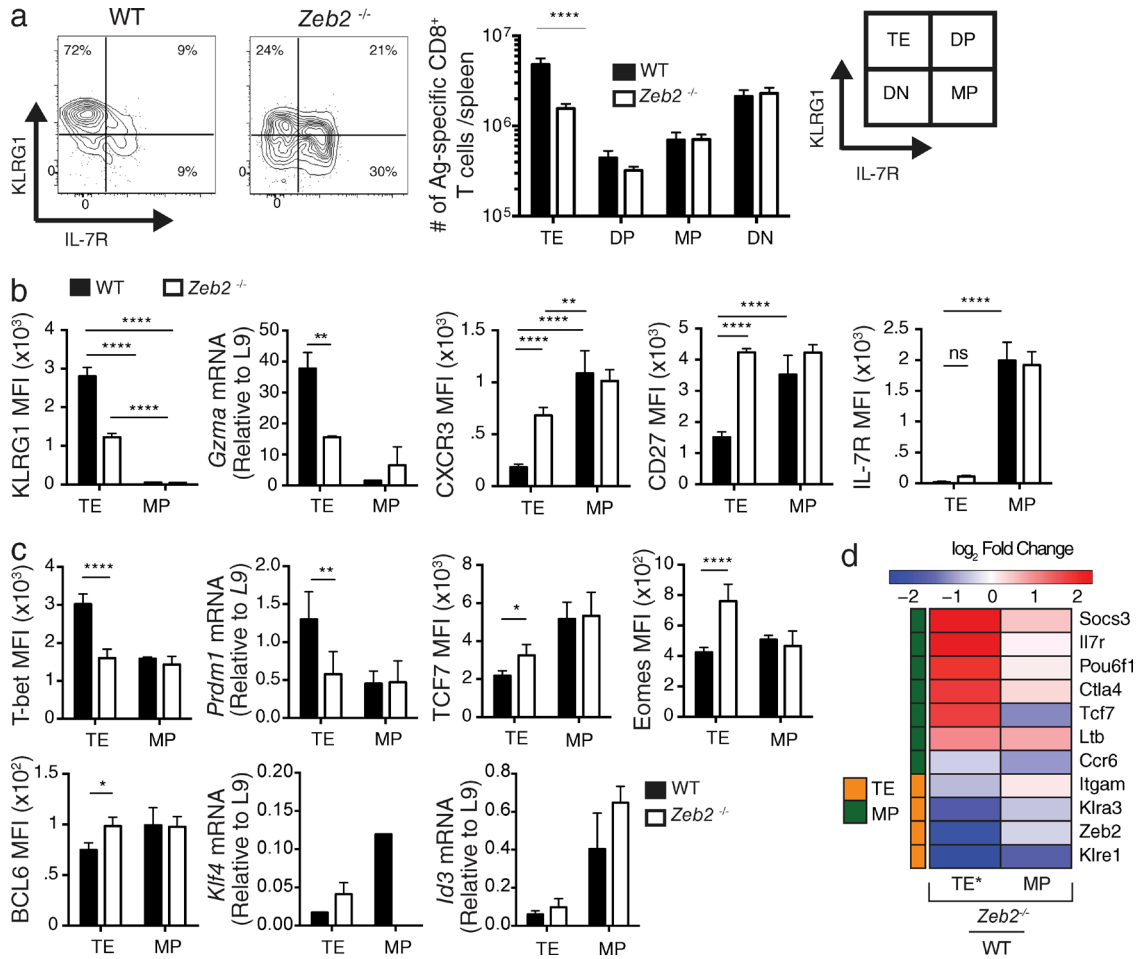
Figure 3. Zeb2⁻/⁻ CTLs are impaired in TE cell differentiation. (a) WT (black) and Zeb2⁻/⁻ (white) mice were infected with LCMV-Arm and the frequency (left plots) and numbers (right bar graph) of tetramer⁺ CTL subsets, as defined by KLRG1 and IL-7R expression was assessed by flow cytometry. Bar graph shows cumulative numbers of D^{b}GP$_{33-41}$- and D^{b}NP$_{396-404}$-specific CTLs combined. (b and c) WT (black bars) or Zeb2⁻/⁻ (white bars) P14 chimeric mice were infected with LCMV-Arm and sacrificed 8 d.p.i. Bar graphs show the expression of several surface and cytotoxic molecules (b) and transcription factors (c) in P14 TE (KLRG1^{hi} IL7R^{lo}) and MP (KLRG1^{lo} IL7R^{hi}) cells as assessed by flow cytometry or qRT-PCR. *, P < 0.05; **, P < 0.01; ****, P < 0.0001. Data are representative of greater than five experiments (n = 4–5 mice/group). (d) WT and Zeb2⁻/⁻ P14 CD8⁺ T cells from 8 d.p.i. were sorted based on KLRG1^{hi} IL7R^{lo} and KLRG1^{lo} IL7R^{hi} expression to normalize according to phenotype. mRNA was isolated from the four sample groups in triplicate and hybridized to Illumina MouseWG-6 v2.0 microarrays to compare differentially expressed genes within each subset between Zeb2⁻/⁻ versus WT cells. Data were analyzed using the limma package in R and a heat map of select top statistically significant (*, FDR < 0.01, Benjamini-Hochberg) differentially expressed MP and TE genes is shown, with statistical significance achieved in the TE subset fold-change (left column). Sidebar denotes MP- (green) and TE-signature (gold) genes.

gration, and adhesion (Fig. 4 f). The codependent gene set affected in both Zeb2⁻/⁻ and Tbx21⁻/⁻ CTLs included known regulators of CTL differentiation, such as Prdm1 (Blimp-1), Runx2, and Tcf7, underscoring the importance of this codependent gene set (Fig. 4 f). Notably, when the codependent gene signature was compared with previously described transcriptional networks of coordinately regulated genes in CD8⁺ T cells, we found that they supported previous predictions of T-bet– and ZEB2-controlled gene networks (Best et al., 2013). Overall, these data suggest T-bet and ZEB2 similar roles in driving terminal CTL differentiation, through the regulation of several pathways, including previously described transcriptional networks.

T–bet binding is enriched in genes dependent on both T–bet and ZEB2 and modulated in the absence of ZEB2

We performed T-bet ChIP-seq to profile genome-wide T-bet binding patterns in WT CTLs 8 d.p.i. In total, there were 9,374 significant T-bet–binding sites (TBS; FDR < 1 × 10⁻⁵) across the genome. These binding sites were annotated to the nearest gene, and comparison to our gene expression data showed that T-bet bound to 48% of TE and 37% of MP cell signature genes (Fig. 5 a). Overall, T-bet bound to 47% of T-bet–dependent genes, which increased to nearly 60% in the ZEB2-dependent and codependent gene sets (Fig. 5 a). This result suggested a bias in T-bet binding and activity at genes co-regulated by ZEB2 and T-bet.
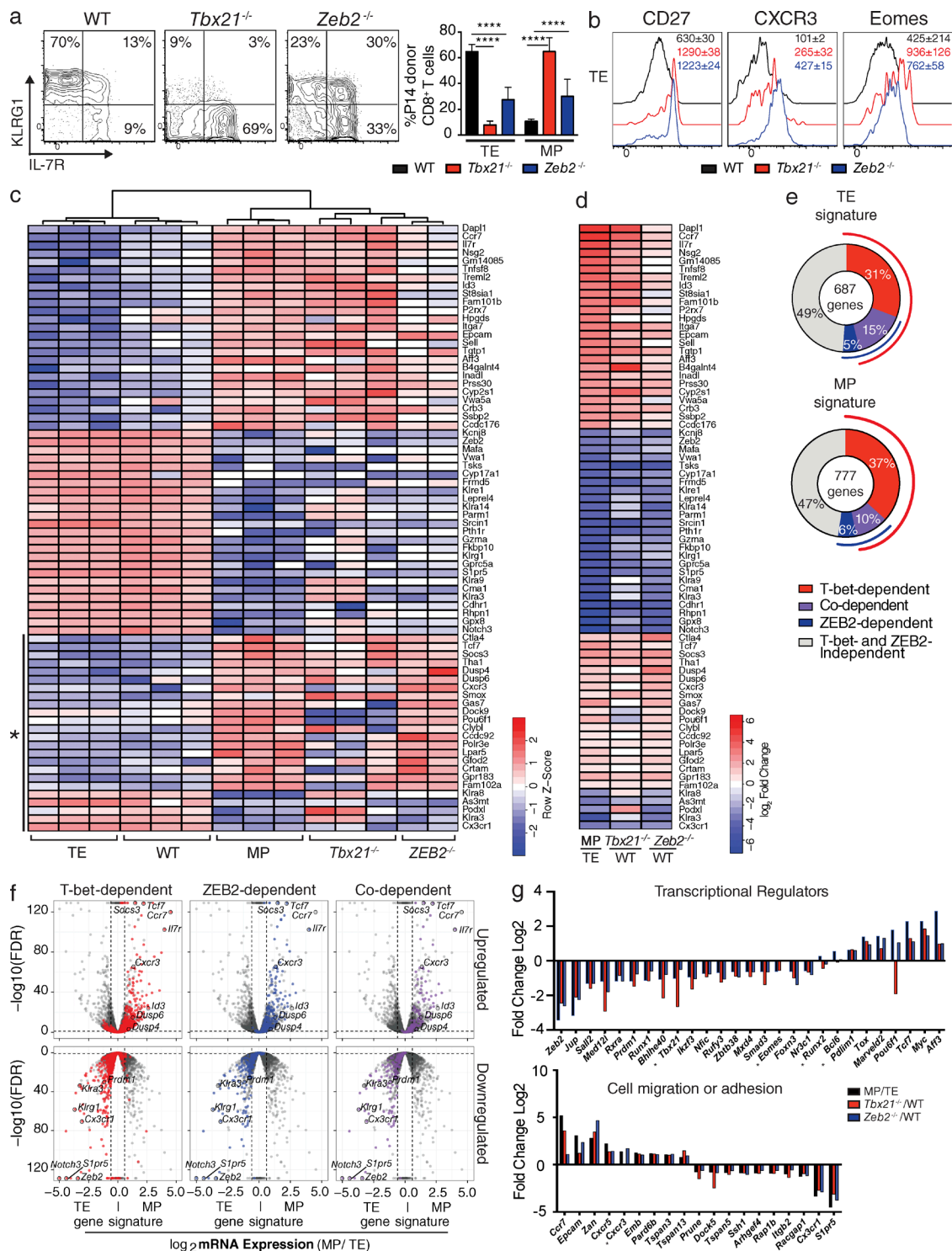
Figure 4. ZEB2 cooperates with T–bet to regulate a subset of genes. (a) Contour plots and bar graph show frequency of subsets, as defined by KLRG1 and IL-7Rα expression in splenic WT, *Zeb2*⁻/⁻, or *Tbx21*⁻/⁻ P14 CTLs 8 d.p.i. (b) Representative histograms show expression of indicated receptor in the respective P14 TE cell population. (c–f) Genome-wide mRNA expression profiling was performed on MP and TE cells as well as total WT, *Tbx21*⁻/⁻, and *Zeb2*⁻/⁻ P14 CD8⁺ T cells at day 8 d.p.i. Differentially expressed genes were defined as ≥1.5 fold different between 2 groups with a FDR of < 0.1. (c) Heat map shows the mRNA expression of the top 50 most differentially expressed genes between MP and TE cell populations, in addition to select biologically relevant genes (*) in these subsets as well as T-bet– and ZEB2-deficient CTLs. (d) Heat map shows the log₂ ratio of MP versus TE cell expression of these genes and how this compares to the differential expression between T-bet⁻/⁻ and *Zeb2*⁻/⁻ versus WT CTLs. (e) Pie graphs show the total numbers of MP- and TE-signature

We then examined whether ZEB2 affected T-bet binding across the genome by performing T-bet ChIP-seq in $Zeb2^{-/-}$ CD8$^+$ T cells isolated at 8 d.p.i. This comparative analysis identified 9787 T-bet binding sites (TBSs) across both sets of samples, of which the majority (94%) were not affected by *Zeb2* deficiency (Fig. 5 b, regions within dotted lines,). However, 136 TBS showed a significant decrease, whereas 413 showed a significant increase in T-bet binding in $Zeb2^{-/-}$ compared with WT CTLs. Interestingly, we observed that several TE-signature loci (gold dots) displayed a loss in both T-bet binding and mRNA expression (Fig. 5, b and c, bottom left quadrant) and, conversely, many MP-signature genes (green dots) displayed an increase in both T-bet binding and gene expression in $Zeb2^{-/-}$ CD8$^+$ T cells (Fig. 5, b and c, top right quadrant). Closer inspection of genes whose expression was dependent on T-bet (red dots), ZEB2 (blue dots), or codependent on both (purple dots) as previously defined (Fig. 4, e and f) showed strong correlations between T-bet binding and mRNA expression in the knockout CTLs (Fig. 5 b, middle and bottom plots).

To confirm the specificity of T-bet binding, we performed motif enrichment analysis at significant TBS common to WT and $Zeb2^{-/-}$ and found, as predicted, a significant central enrichment of known T-box motifs, T and Eomes (Fig. 5 d, top; Teo et al., 2011; Mathelier et al., 2014). Moreover, this was confirmed by performing a de novo motif search, which revealed a significant enrichment of a GSTGTGR motif (E-value = 4.6×10^{-83}) that most closely resembles the T motif (E-value = 4.5×10^{-2}; Fig. 5 d, bottom). Interestingly, Runx1- and Runx2-binding sites also appear to be enriched at TBS, which is in agreement with previous studies showing functional interactions between these transcription factors (Lazarevic et al., 2011), but also resemble T-box motifs in their consensus binding to G(G)TGTG sequences.

Next, we sought to examine computationally if ZEB2 or other transcription factors may bind coordinately with T-bet at certain loci associated with CTL differentiation by performing motif enrichment analysis of the differentially bound T-bet sites between WT and *Zeb2*-deficient CD8$^+$ T cells (see diagram in Fig. 5 e). The most significantly enriched motif discovered within DNA regions associated with *decreased* T-bet binding (WT > $Zeb2^{-/-}$) was a KTGTGA motif (E-value = 3×10^{-3}), which most resembles the T motif (E-value = 0.026; Fig. 5 e). In contrast, the most significantly enriched motif discovered within the DNA regions associated with increased T-bet binding ($Zeb2^{-/-}$ > WT) was a CAGGTRW motif (E-value = 6.5×10^{-29}), which most highly resembles the ZEB1 and ZEB2 E-box DNA binding domain motif (Comijn et al., 2001; Fig. 5 e). Lastly, sites with increased T-bet binding containing the CAGGTRW motif were identified and showed significant overlap with MP genes up-regulated in $Zeb2^{-/-}$ (Fig. 5 f). One could infer from these computational correlations that ZEB2 and T-bet coordinately bind to several MP-signature gene loci, and that ZEB2 is required to both restrict T-bet binding and to repress transcriptional activation of these genes. Direct testing of this hypothesis requires the ability to ChIP ZEB2, which is not feasible at this time.

T–bet regulation of several MP and TE genes is ZEB2 dependent

The gene expression profiling experiments showed that ZEB2 and T-bet regulate the expression of a common set of genes in CTLs (Fig. 4, c–f), and the T-bet ChIP-seq data suggested ZEB2 influences T-bet binding to its targets (Fig. 5, b–f). However, considering that ZEB2 is necessary for maximal T-bet expression, and that T-bet binding to the *Tbx21* locus is somewhat lower in $Zeb2^{-/-}$ CTLs (Figs. 3 c and 5 c), it was still unclear whether ZEB2 mainly acted to promote T-bet expression or whether ZEB2 itself was directly necessary for the regulation of CTL gene expression.

To further address the cooperative functions between ZEB2 and T-bet, we overexpressed (OE) T-bet in WT and $Zeb2^{-/-}$ P14 CTLs using a T-bet expressing retrovirus (RV) and determined whether *Zeb2* was necessary for the ability of T-bet to induce or repress TE- and MP-signature genes in CTLs during LCMV infection (Fig. 6, a and b). Intracellular staining for T-bet protein showed that it was expressed to a similar extent in both WT and $Zeb2^{-/-}$ P14 CTLs transduced with T-bet RV (Fig. 6 c). T-bet OE sufficiently induced expression of KLRG1 in both WT and *Zeb2*-deficient CTLs, and thus KLRG1^{hi} TE-like cells were sorted to compare gene expression genome-wide using RNA-seq. This showed that when T-bet was OE in WT CTLs, it further enhanced expression of *S1pr5*, *Zeb2*, *Notch3*, and *Cx3cr1* above and beyond that of the empty vector control cells (Fig. 6 a, compare columns 1 and 2). T-bet OE could also intensify repression of certain MP genes such as *Cxcr3*, *Tcf7*, *Eomes*, *Ltb*, *IL-7r*, and *ccr7* in WT KLRG1^{hi} CTLs compared with empty vector control cells (Fig. 6 a, compare columns 1 and 2). However,

genes subdivided by the frequency of genes that are dependent on T-bet (red), ZEB2 (blue), or both (codependent, purple) for normal expression. (f) Volcano plots show differential expression of MP and TE signature genes. Genes up-regulated (top) or down-regulated (bottom) in $Tbx21^{-/-}$ CTLs (red), $Zeb2^{-/-}$ CTLs (blue), or in both (purple) are highlighted. A few genes of biological significance genes are highlighted. (g) The MP and TE signature genes were subdivided into functional categories as indicated, based on known or predicted functions (e.g., transcriptional regulators, cell adhesion/migration). Bar graphs show the fold change (log$_2$ ratio) of differentially expressed genes between MP and TE, $Tbx21^{-/-}$ and WT, as well as $Zeb2^{-/-}$ and WT CTLs ($\geq$1.5-fold change with a FDR $\leq$ 0.1). * denote biologically relevant genes that were either not differentially expressed, or not statistically significant. Data are representative of four independent experiments (n = 4–5 mice/group) in a and b and two ($Zeb2^{-/-}$ CTLs) or three (all other groups) independent biological replicates (c–f; n = 4–5 mice/group/replicate). Bars represent mean expression $\pm$ SEM. ****, P < 0.0001.
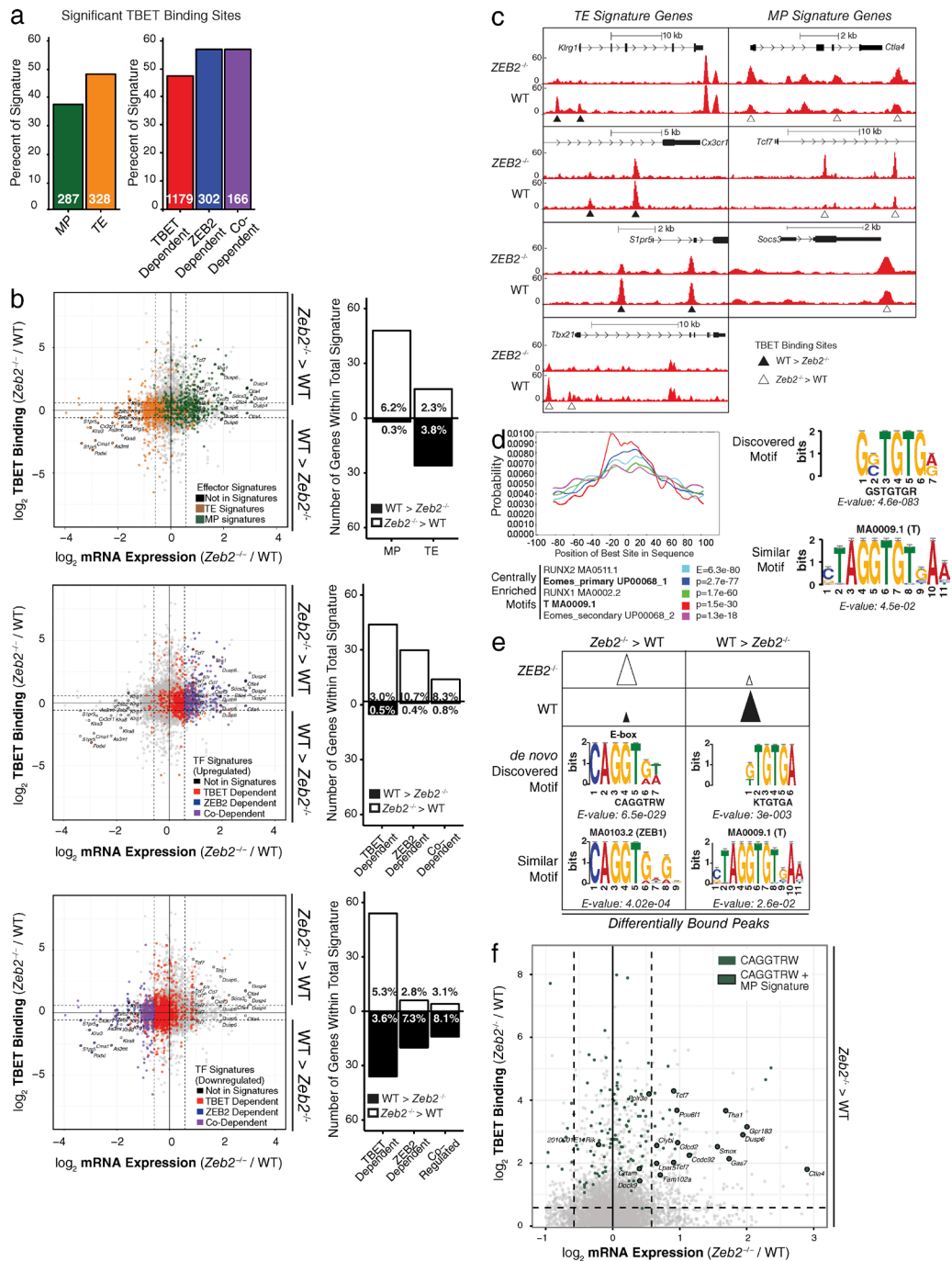
Figure 5. **ZEB2 is required for normal amounts of T-bet binding at several TE genes that are codependent on T-bet and ZEB2.** Total P14 CTLs were purified at 8 d.p.i. and samples were processed for T-bet ChIP-Seq in WT and $Zeb2^{-/-}$, as described in Materials and methods. (a) Bar graphs show the frequency of genes in the indicated gene signature sets (with number of genes inscribed) annotated to contain TBSs as determined based on the MACS v2.1.0 analysis (FDR < 1 × 10^{-5}). (b–e) TBSs were annotated to the nearest gene and compared between WT and $Zeb2^{-/-}$ CTLs for differential T-bet binding (FDR < 1 × 10^{-5}). TBS displaying decreased or increased T-bet binding in $Zeb2^{-/-}$ versus WT cells were categorized as WT > $Zeb2^{-/-}$ or $Zeb2^{-/-}$ > WT, respectively. (b) Scatter plots quantitate the log$_2$ fold-change in T-bet binding versus the log$_2$ fold-change in mRNA expression in $Zeb2^{-/-}$ versus WT. Dashed lines designate fold-changes of 1.5; bar graphs to right show the number of genes within each signature (with frequency inscribed) that display increased (white bar) or decreased (black bar) T-bet binding in $Zeb2^{-/-}$ relative to WT cells. Genes contained within the MP (green), TE (gold), T-bet-dependent (red), ZEB2-dependent (blue), or codependent (purple) gene signatures are shown. (c) T-bet ChIP-seq tracks from $Zeb2^{-/-}$ and WT CTLs at select MP and TE loci are shown with differential TBS identified below the tracks. (d) Motif discovery and enrichment analysis of DNA sequences flanking the summits of TBS common between WT and $Zeb2^{-/-}$ CD8 T cells identified several known centrally enriched motifs that included T-box consensus sequences for Eomes and T

in the absence of *Zeb2*, T-bet OE was largely ineffective at altering gene expression at the majority of MP- and TE-signature genes (Fig. 6 a, compare columns 2 and 4), as well as genome-wide (Fig. 6 b). We refer to this category of genes (clusters I and II) as *Zeb2* dependent. Of course, there were some *Zeb2*-independent genes (clusters III and IV) whose expression could be altered by T-bet OE in the absence of *Zeb2*, but this was a minority of genes (Fig. 6, a and b). The effects of T-bet OE on protein expression in WT and *Zeb2*-deficient CTLs were confirmed for a subset of genes by flow cytometry (Fig. 6 c). These data showed quite strongly that T-bet and ZEB2 act in a cooperative, nonredundant manner because T-bet was heavily dependent on *Zeb2* for its ability to repress a large number of MP-signature genes and, more surprisingly, to induce the many TE-signature genes in KLRG1^{hi} CTLs. Thus, in addition to augmenting T-bet protein levels in TE cells, ZEB2 is also necessary downstream of or in conjunction with T-bet to drive the transcriptional programming of terminal differentiation in CD8^{+} T cells.

DISCUSSION

During infection, the adaptive immune response has two primary goals; a short-term goal of eradicating the present infection and a long-term goal of establishing immunological memory, all of which needs to occur without excessive collateral damage to host tissues. Elucidating the factors that control effector T cell differentiation to fulfill these two goals is essential for understanding how long-lived immunity to pathogens forms and potentially allowing for therapeutic manipulation of effector and memory CD8^{+} T cell function. Previous work identified T-bet as a central regulator of terminal differentiation in CD8^{+} T cells, which operates in a graded manner with higher amounts driving TE and lower amounts supporting MP cell differentiation (Takemoto et al., 2006; Joshi et al., 2007). In this study, we found that high amounts of T-bet induced *Zeb2* mRNA expression and that ZEB2 was critical for the transcriptional programming of TE cell differentiation. To our knowledge, this study, along with that of Omilusik et al. (2015), is the first to describe the function of ZEB2 in T cells. Overall, these data suggest that ZEB2 and T-bet enforce terminal effector differentiation through their cooperation by simultaneously inducing TE and repressing MP cell gene expression. Thus, this study not only identifies a novel regulator of TE fates, but also provides new insights into the mechanisms by which graded T-bet drives terminal effector differentiation through its cooperative functions with ZEB2.

The differentiation of stem cells into specialized cell types with distinct functions and phenotypes involves the activation of differentiation genes and the suppression of stemness genes (Bernstein et al., 2006; Sánchez Alvarado and Yamanaka, 2014). A similar process occurs in CD8^{+} T cells as terminal effector cells develop apart from memory precursor CD8^{+} T cells, and this study has identified key roles for T-bet and ZEB2 in controlling these differentiation programs. Given that ZEB2 has primarily been described as a transcriptional repressor, known to recruit histone deacetylases (Verstappen et al., 2008; Wang et al., 2009; Kim et al., 2012), we predicted that ZEB2 would repress MP cell genes and this was confirmed by analysis of gene expression in *Zeb2*^{−/−} KLRG1^{hi} CTLs. Based on the data presented herein, we postulate that once T-bet levels surpass a given threshold, T-bet switches on ZEB2, and then T-bet and ZEB2 bind in a coordinated fashion at certain MP regulatory loci to mediate their repression. This model is supported by the proximity and overlap of ZEB1/2 and T-box motifs in TBS at several MP loci that are derepressed in *Zeb2*^{−/−} TE-like cells. Several of these loci displayed both increased T-bet binding and expression in *Zeb2*-deficient CTLs, and their mRNA expression was further augmented by T-bet OE. These data suggest that ZEB2 may serve dual roles at distinct MP loci by both restricting T-bet binding and recruiting gene silencing machinery. Possibly T-bet directly recruits ZEB2 to such loci similar to the model recently proposed for transcriptional repressor Bcl6 (Oestreich et al., 2011). It is worth noting that some of these MP genes that show both increased T-bet binding and mRNA expression in *Zeb2*^{−/−} CTLs are also increased in expression in the absence of T-bet, suggesting increased T-bet binding is not necessary for their expression. One possibility is that, the T-box TF homologue of T-bet, Eomesodermin, acts redundantly to promote MP signature gene expression in *Tbx21*^{−/−} CD8 T cells.

A potential caveat with the experiments comparing T-bet binding between WT and *Zeb2*^{−/−} CTLs is that the two populations contained different frequencies of TE and MP cells, and this may have biased the results. We argue that this confounding issue is likely insignificant because T-bet binds to ∼35% of MP-signature genes in CTLs, yet only 6% of these genes demonstrated significant gains in T-bet binding in the absence of *Zeb2* (if this was simply an artifact of overrepresentation of MP cells in the *Zeb2*^{−/−} cell population, one would expect that all of the MP cell loci with TBSs would have shown increased T-bet binding). Moreover, many of the TBSs that showed increased binding in *Zeb2*^{−/−} cells also contained predicted ZEB2-binding sites, yet this was not observed in the TE genes that displayed decreased T-bet binding in *Zeb2*^{−/−} cells. Thus, there was a selectivity of in-

---

(i.e., brachyury or T-box) in addition to Runx1/2. Line graph (top) notes positions of indicated motifs. De novo motif discovery was performed in parallel on the TBS and the most significantly enriched motif (GSTGTGR) along with its most similar motif (T) is shown (bottom). (e) Motif discovery and enrichment analysis was performed among the differential TBS between WT and *Zeb2*^{−/−} CD8 T cells (*Zeb2*^{−/−} > WT or WT > *Zeb2*^{−/−}), as diagrammed. The most highly enriched motif discovered and the E-value of enrichment are shown along with its most similar motif and its corresponding E-value. (f) Scatter plot from panel b highlighting loci containing the CAGGTRW discovered by motif enrichment analysis as putative ZEB2-binding sites.
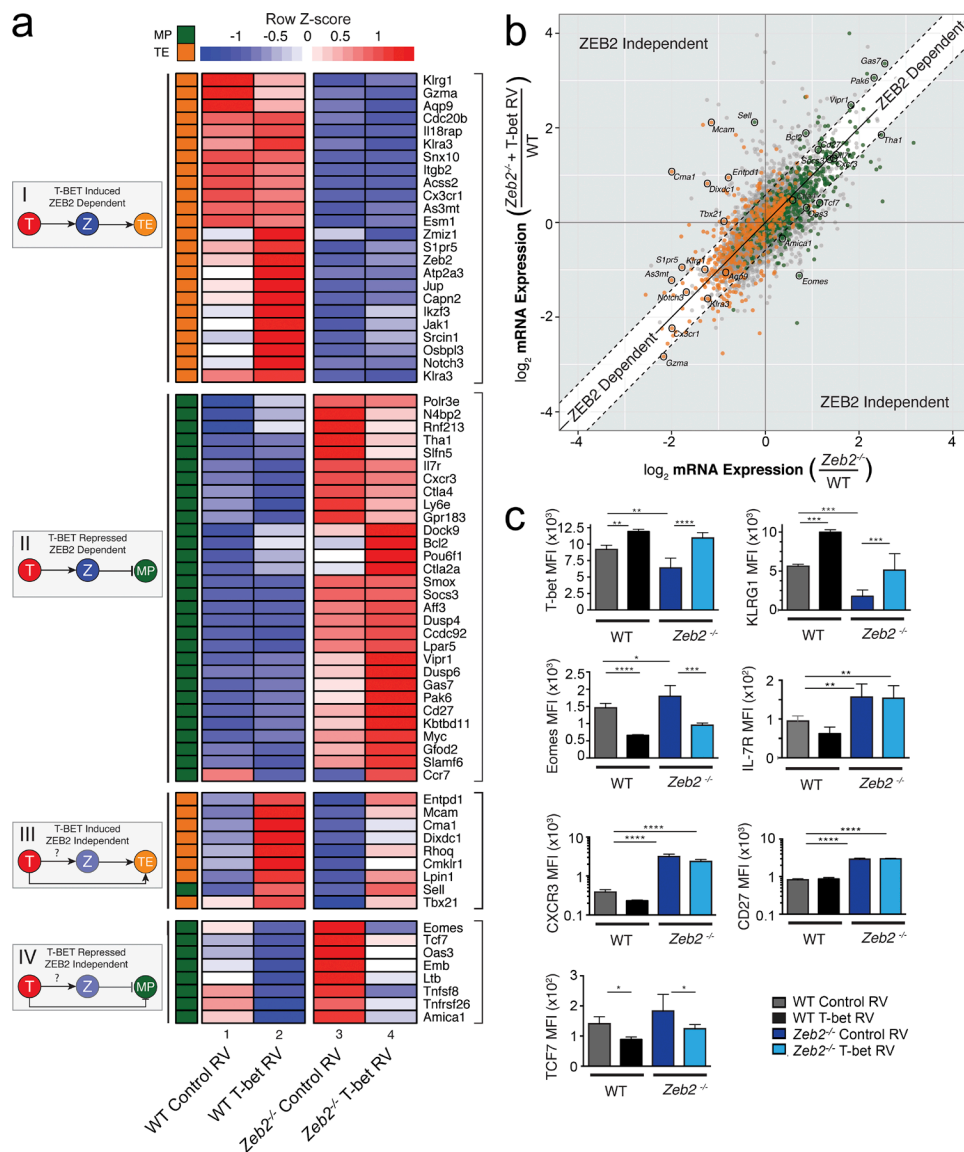
Figure 6. ZEB2 is necessary for the regulation of several MP and TE–signature genes. WT or *Zeb2$^{-/-}$* P14 CD8$^+$ T cells were transduced with MigR1 retroviruses (RVs) overexpressing T-bet (T-bet RV) or empty control RVs, which generated four experimental groups. After transduction, 10^5 P14 CTLs were transferred into naive B6 recipients that were subsequently infected with LCMV-Arm, and 8 d.p.i. the RV-infected *KLRG1^{hi}* P14 CTLs were sorted and processed for RNA-seq (a and b) or the *total* RV-infected P14 CTL population was examined for expression of particular receptors and transcription factors by flow cytometry (c). (a) Heat map shows genes within the MP and TE signatures that are induced or repressed by T-bet, and operate in either a ZEB2-dependent or -independent manner. Genes are divided into four clusters (I–IV) highlighting these different models of regulation (right of heat map). (b) Scatter plot of mRNA expression between *Zeb2$^{-/-}$* versus WT (x-axis) and *Zeb2$^{-/-}$* + T-bet RV versus WT (y-axis). Solid diagonal line represents the similarity of gene expression and the dashed lines show division of genes for which T-bet overexpression increased or decreased expression by ±1.5-fold-change. Thus, genes in gray sections represent those in which T-bet could induce or repress independent of ZEB2 and genes in white section, along solid diagonal line, represent those in which T-bet was dependent on ZEB2 to modulate. MP- and TE-signature genes are highlighted with green and gold colors (a and b). (c) Representative bar graphs show protein expression in the four groups of CTLs as assessed by flow cytometry. Data are representative of three (a–b) and four (c) independent experiments (*n* = 4–5 mice/group). Bars represent mean expression ± SEM. *, P < 0.05; **, P < 0.01; ***, P < 0.001; ***, P < 0.0001; ****, P < 0.0001.

creased T-bet binding at MP loci that also had neighboring predicted ZEB2-binding sites. Rigorous molecular testing of this model in murine T cells would require better reagents to study ZEB2 protein, or possibly future studies in human T cells to determine the conservation of ZEB2 function.

The *Zeb2$^{-/-}$* CTL phenotype does not simply reflect a reduction in T-bet protein, as T-bet overexpression could not fully restore the TE cell genetic program. Rather, we find that *Zeb2* is a necessary downstream mediator of T-bet activity in driving terminal effector cell differentiation. As

T-bet overexpression failed to induce several TE-cell signature genes in the absence of *Zeb2*, this suggests that ZEB2 is necessary to either (a) repress a pro–memory transcriptional repressor that restricts TE-signature gene expression (e.g., Bcl6) or (b) it has an alternative function as a transcriptional activator in TE cells. Indeed, there are reports that ZEB2 can act as a transcriptional activator when complexed with SP1, driving the expression of vimentin and integrin α-5 in certain cancer cell lines without directly binding DNA (Bindels et al., 2006; Nam et al., 2012).

An interesting observation made during the course of this study was that *Zeb2* mRNA remained elevated in the subset of KLRG1$^+$ IL-7R$^+$ T$_{EM}$ cells after effector cell contraction. Although cells of this phenotype display a limited lifespan and proliferative capacity compared with KLRG1^{lo} IL-7R^{hi} memory CD8$^+$ T cells in circulation, they can offer enhanced protection to some types of pathogens due to elevated cytotoxic activity (Jabbari and Harty, 2006; Olson et al., 2013) and, interestingly, are more prominently observed after serial infections (Masopust et al., 2006; Wirth et al., 2010; Joshi et al., 2011; Fraser et al., 2013; Olson et al., 2013). Thus, it will be important to determine if sustained ZEB2 expression is necessary for maintenance of this population of T$_{EM}$ cells. Furthermore, *Zeb2* mRNA levels are elevated in CD8$^+$ T cells during chronic LCMV infection (Doering et al., 2012) and reduced in T$_{RM}$ cells relative to circulating T$_{EM}$ cells (Wakim et al., 2012; Mackay et al., 2013; Tse et al., 2013). Perhaps *Zeb2* mRNA is repressed in T$_{RM}$ cells because it enhances CTL expression of *Cx3cr1* and *S1pr5*, which may affect the tissue-restricted localization of T$_{RM}$ cells. In the future, it will be of great interest to uncover the role of ZEB2 in regulating CTL differentiation in different tissues and settings of infection. Moreover, ZEB2 is also expressed in CD4$^+$ T cells, NK cells, monocytes, and other immune cells, and it might function in a similar manner, possibly in cooperation with T-bet, to promote terminal differentiation of other lymphocytes. Elucidating the genetic pathways that switch on terminal differentiation in T cells will enhance our understanding of how specialized types of T cells are established and stabilized during immune responses, which could inform therapies aimed at enhancing effective CTL memory development.

MATERIALS AND METHODS

Mice. C57BL/6 (B6) mice were obtained from the National Cancer Institute (Frederick, MD). *Zeb2$^{flox/flox}$* mice were originally generated by D. Hoylebroeck (University of Leuven, Leuven, Belgium; Higashi et al., 2002) and obtained from R. Aslopp (John A. Burns School of Medicine, University of Hawaii, Honolulu, HI). Granzyme B-Cre (GzB-Cre$^+$) mice were provided by J. Jacobs (Emory University, Atlanta, GA) via R. Flavell's laboratory (Yale University School of Medicine, New Haven, CT) and were crossed to *Zeb2$^{flox/flox}$* mice for generation of GzB-cre$^+$; *Zeb2$^{flox/flox}$* (*Zeb2$^{-/-}$*) mice and GzB-cre$^+$; *Zeb2$^{+/+}$* or GzB-cre$^-$; *Zeb2$^{flox/flox}$* (*Zeb2$^{+/+}$*) mice.

Zeb2$^{-/-}$ and *Zeb2$^{+/+}$* mice were further crossed to P14 TCR transgenic mice so that P14 *Zeb2$^{-/-}$* and P14 *Zeb2$^{+/+}$* mice could be obtained. To generate "P14 chimeric mice" 10–50,000 P14 CD8$^+$ T cells were transferred into B6 mice by i.v. injection. All animal experiments were done with approved institutional animal care and use committee protocols.

Infections and treatments. For infections of mice, 2×10^5 PFU of the LCMV Armstrong strain were administered i.p. For recall experiments, mice were infected with 2×10^6 PFU of the LCMV clone 13 strain i.v. by retroorbital injection. Viral titers were measured by plaque assay (Wherry et al., 2003a).

For BrdU labeling to determine homeostatic proliferation, BrdU (1 mg/ml) was administered in the drinking water daily for 10 d.

Antibodies for surface and intracellular staining. Lymphocyte isolation, along with surface and intracellular staining, was performed as described previously (Joshi et al., 2007). For in vitro stimulation, splenocytes were stimulated with GP$_{33-41}$ and GP$_{NP396-404}$, peptides (100 ng/ml) for 5 h in the presence of Brefeldin A. Antibodies were purchased from eBioscience, BD, or BioLegend and Cell Signaling Technology. Class I MHC tetramers were generated as described previously (Kaech et al., 2003). Anti-BRDU antibody was purchased from BD and used according to instructions. Flow cytometry data were acquired on BD LSRII with Diva software and analyzed with Flow Jo software (Tree Star). Sorting was performed on a FACS Aria (BD).

Cytotoxicity assays. Naive splenocytes were isolated from B6 mice and either labeled with 1 µM CFSE and pulsed with GP$_{33-41}$ (100 ng/ml) or labeled with 0.1 µM CFSE alone. In total, 5 million of each target cell population were adoptively transferred i.v. to day 8 LCMV-infected WT or *Zeb2$^{-/-}$* mice. 1 h later, the mice were sacrificed and flow cytometry was used to determine the presence of transferred cells in the spleen.

ChIP and ChIP-sequencing (ChIP-seq). ChIP experiments were performed on Thy1.1 P14 CTLs enriched by selection of the congenic marker Thy1.1 from 8 d.p.i. splenocytes using Easy Sep biotin selection kits (STEMCELL Technologies Inc.) in conjunction with anti-Thy1.1 mAbs (eBioscience). Sample purity was >90%.

One additional sample (Fig. 1 e) was stimulated with IL-12 (10 ng/ml) to enhance T-bet expression. Chromatin was recovered from batches of 10 million cells, after cross-linking with 1% formaldehyde for 10 min and sonication to obtain DNA fragment ~200–500 bp. ChIP was performed with anti–T-bet (Santa Cruz Biotechnology, Inc.) from 20 million cells chromatin was isolated, amplified, and processed into a library. Illumina HiSeq 2000 was used for sequencing. Sequence reads from each cDNA library (paired-end, 75 bp) were mapped onto the mouse genome build mm10 using bowtie2.

Conventional ChIP was performed as described but anti–mouse IgG was used as a negative control. Three independent experiments were performed. Immunoprecipitated DNA was analyzed by qPCR. Sybr-based qPCR was performed with the following primers: *Ifng* promoter forward, 5′-GCTTTCAG AGAATCCCACAAGAAT-3′, *Ifng* promoter reverse, 5′-GCT ATGGTTTTGTGGCATGTTAGA-3′; *Zeb2*TSS promoter forward: 5′-CGGCTGCTTCATTGATAAGA-3′, *Zeb2*TSS promoter reverse: 5′-CGCTGTGTTTGGTTGCTAGA-3′; *Zeb2* 3-kb upstream forward: 5′-GATGCAGGGGGCT GATTAT-3′, *Zeb2* 3kb upstream reverse: 5′-CCCCCTTT TGTGAGACTGA-3′; *Il-7r* promoter forward: 5′-TTG CTGCTACCAATCAGTAAGAAT-3′, *Il-7r* promoter reverse: 5′-TGGGGCTCTTTTACGAGTGA-3′.

Differential binding analysis and quantification of ChIP-Seq. Using the MACS v2.1.0 peak caller (Feng et al., 2012), peaks were first called relative to input using the *callpeak* module with the *−B,−nomodel*, and *−extsize 200* options set. Peaks from replicates within groups were intersected to identify consensus peaks, and then the union of peaks between groups was taken to serve as features used for further analysis. To identify differential binding events, these features were quantified for signal using the bedgraph output and bedtools map utility to sum the reads normalized for sequencing depth over the enriched regions. HOMER2 was then used to annotate the peaks to the nearest gene using the GRCM38 (mm10) reference genome. All processing thereafter was performed in R, importing the annotated peaks and tag quantification per peak. For the purpose of visualization, the two replicates per group (WT and *Zeb2*−/−) were pooled and visualized using the UCSC Genome Browser.

Motif enrichment analysis. Motif enrichment analysis was performed using the MEME 4.10 suite of tools. Genomic sequences at the summit of T-bet binding peaks ±100 bp were analyzed for central enrichment using Centrimo. 200 bp genomic sequences of regions identified as differentially bound were compared against a background of sites with no differential binding (common) to search for the enrichment of de novo motifs. Using the DREME algorithm with default settings on each group, discovered motifs were then submitted to Tomtom to find the most similar motif for each de novo motif. For the CAGGTRW motif enriched in the *Zeb2*−/− >WT group, sites containing this motif were identified using the FIMO algorithm, and visualized using R.

Retroviral transduction. Viral supernatants for the retroviral constructs described in these studies were obtained by transfection of 293T cells with the respective retroviral construct and Eco-helper. Transfections were performed using Fugene6 (Promega) or Xtremegene9 (Roche); no difference was noted in transfections performed with these reagents. P14 donor mice were directly infected with 2 × 10⁶ PFU LCMV-Armstrong i.v. and, 1 d later, mice were sacrificed and splenocytes

were isolated. Splenocytes were spin-transduced for 90 min at 34°C with viral supernatant in the presence of 8 µg/ml polybrene. After transduction, 0.5–1 × 10⁵ P14 CTLs were transferred i.v. to recipient mice B6 mice that were subsequently infected with 2 × 10⁵ PFU LCMV i.p.

Gene expression by qRT-PCR. For qRT-PCR, RNA was isolated from 200,000–1,000,000 sorted cells by QIAshredder and RNeasy kits (QIAGEN); the use of QIAzol and RWT buffers with the RNeasy kits; or TRIzol extraction (Life Technologies) followed by ethanol precipitation. CDNA was synthesized using SSRTII (Life Technologies) and qRT-PCR was performed on a Stratagene Mx3000P with iTaq Universal SYBR Green super mix (Bio-Rad Laboratories). Relative fold changes were calculated using *Rpl9* (*L9*) expression.

The following primers were used in these studies: *Zeb2* forward: 5′-GAGCAGGTAACCGCAAGTTC-3′ *Zeb2* reverse: 5′-TGTTTCTCATTCGG-3′; *Rpl9* forward: 5′-TGA AGAAATCTGTGGGTCG-3′ *Rpl9* reverse: 5′-GCACTACG GACATAGGAACTC-3′; *Prdm1* forward: 5′-GACGGGGGG TACTTCTGTTCA-3′ *Prdm1* reverse: 5′-GGCATTCT TGGGAACTGTGT-3′; Eomes forward: 5′-ATGTACGT TCACCCAGAATC-3′ Eomes reverse: 5′-GTGCAGAG ACTGCAACACTA-3′S; Klf4 forward: 5′-CCACACTT GTGACTATGCAG-3′ Klf4 reverse: 5′-CCAGTCACAGTGG TAAGGTT-3′ Cxcr3; forward: 5′-CAGCCAAGCCATG TACCTTGAG-3′ Cxcr3 reverse: 5′-TCAGGCTGAAATC CTGTGGGCA-3′; Id3 forward: 5′-ACTTACCCTGAAC TCAACGC-3′ Id3 reverse: 5′-CTCCAAGGAAACCAGAAG AA-3′; Tbx21 forward: 5′-CAACAACCCCTTTGCCAA AG-3′ Tbx21 reverse: 5′-TCCCCCAAGCAGTTGACAGT-3′; Gzma forward: 5′-TCAGCTCCCTCTGAAACTCT-3′ Gzma reverse: 5′-TCTCCACCAAAAGAGGTGAT-3′.

RNA-seq library preparation and data analysis. Total RNA was purified with the use of QIAzol and RNeasy Mini kit (QIAGEN), in which an on-column DNase treatment was included. Purified RNA was submitted to the Yale Center for Genomic Analysis where it was subjected to mRNA isolation and library preparation. Libraries were pooled, six samples per lane, and sequenced on an Illumina HiSeq 2500 (75-bp paired end reads), and aligned using STAR to the GRCm38 (mm10) reference genome. A count-based differential expression protocol was adapted for this analysis (Anders et al., 2013); mappable data were counted using HTSeq, and imported into R for differential expression analysis using the DESeq2. To find differentially regulated sets of genes for signature generation, an absolute 1.5-fold-change difference between samples and FDR (Benjamini–Hochberg) ≤ 0.1 was used.

Statistical analysis. Prism 6 (GraphPad Software) was used to calculate statistics for all bar graphs shown. For comparisons of two groups, two-tailed Student's *t* test was performed. For multiple group comparisons, one-way ANOVA was used with Tukey's multiple comparisons test. For grouped multiple

comparisons two-way ANOVA with Sidak's multiple comparison test was used. *, P < 0.05; **, P < 0.01; ***, P < 0.001; and ****, P < 0.0001.

REFERENCES

Ahmed, R., and D. Gray. 1996. Immunological memory and protective immunity: understanding their relation. *Science.* 272:54–60. http://dx.doi.org/10.1126/science.272.5258.54

Anders, S., D.J. McCarthy, Y. Chen, M. Okoniewski, G.K. Smyth, W. Huber, and M.D. Robinson. 2013. Count-based differential expression analysis of RNA sequencing data using R and Bioconductor. *Nat. Protoc.* 8:1765–1786. http://dx.doi.org/10.1038/nprot.2013.099

Arsenio, J., B. Kakaradov, P.J. Metz, S.H. Kim, G.W. Yeo, and J.T. Chang. 2014. Early specification of CD8⁺ T lymphocyte fates during adaptive immunity revealed by single-cell gene–expression analyses. *Nat. Immunol.* 15:365–372. http://dx.doi.org/10.1038/ni.2842

Barbu, E.A., J. Zhang, E.H. Berenstein, J.R. Groves, L.M. Parks, and R.P. Siraganian. 2012. The transcription factor Zeb2 regulates signaling in mast cells. *J. Immunol.* 188:6278–6286. http://dx.doi.org/10.4049/jimmunol.1102660

Bernstein, B.E., T.S. Mikkelsen, X. Xie, M. Kamal, D.J. Huebert, J. Cuff, B. Fry, A. Meissner, M. Wernig, K. Plath, et al.. 2006. A bivalent chromatin structure marks key developmental genes in embryonic stem cells. *Cell.* 125:315–326. http://dx.doi.org/10.1016/j.cell.2006.02.041

Best, J.A., D.A. Blair, J. Knell, E. Yang, V. Mayya, A. Doedens, M.L. Dustin, and A.W. Goldrath; Immunological Genome Project Consortium. 2013. Transcriptional insights into the CD8⁺ T cell response to infection and memory T cell formation. *Nat. Immunol.* 14:404–412. http://dx.doi.org/10.1038/ni.2536

Bindels, S., M. Mestdagt, C. Vandewalle, N. Jacobs, A. Volders, A. Noël, F. van Roy, G. Berx, J.-M. Foidart, and C. Gilles. 2006. Regulation of vimentin by SIP1 in human epithelial breast tumor cells. *Oncogene.* 25:4975–4985. http://dx.doi.org/10.1038/sj.onc.1209511

Cho, J.Y., V. Grigura, T.L. Murphy, and K. Murphy. 2003. Identification of cooperative monomeric Brachyury sites conferring T-bet responsiveness to the proximal IFN-gamma promoter. *Int. Immunol.* 15:1149–1160. http://dx.doi.org/10.1093/intimm/dxg113

Comijn, J., G. Berx, P. Vermassen, K. Verschueren, L. van Grunsven, E. Bruyneel, M. Mareel, D. Huylebroeck, and F. van Roy. 2001. The two-handed E box binding zinc finger protein SIP1 downregulates E-cadherin and induces invasion. *Mol. Cell.* 7:1267–1278. http://dx.doi.org/10.1016/S1097-2765(01)00260-X

Cui, W., Y. Liu, J.S. Weinstein, J. Craft, and S.M. Kaech. 2011. An interleukin-21-interleukin-10-STAT3 pathway is critical for functional maturation of memory CD8⁺ T cells. *Immunity.* 35:792–805. http://dx.doi.org/10.1016/j.immuni.2011.09.017

Doering, T.A., A. Crawford, J.M. Angelosanto, M.A. Paley, C.G. Ziegler, and E.J. Wherry. 2012. Network analysis reveals centrally connected genes and pathways involved in CD8+ T cell exhaustion versus memory. *Immunity.* 37:1130–1144. http://dx.doi.org/10.1016/j.immuni.2012.08.021

Feng, J., T. Liu, B. Qin, Y. Zhang, and X.S. Liu. 2012. Identifying ChIP-seq enrichment using MACS. *Nat. Protoc.* 7:1728–1740. http://dx.doi.org/10.1038/nprot.2012.101

Fraser, K.A., J.M. Schenkel, S.C. Jameson, V. Vezys, and D. Masopust. 2013. Preexisting high frequencies of memory CD8⁺ T cells favor rapid memory differentiation and preservation of proliferative potential upon boosting. *Immunity.* 39:171–183. http://dx.doi.org/10.1016/j.immuni.2013.07.003

Goossens, S., V. Janzen, S. Bartunkova, T. Yokomizo, B. Drogat, M. Crisan, K. Haigh, E. Seuntjens, L. Umans, T. Riedt, et al.. 2011. The EMT regulator Zeb2/Sip1 is essential for murine embryonic hematopoietic stem/progenitor cell differentiation and mobilization. *Blood.* 117:5620–5630. http://dx.doi.org/10.1182/blood-2010-08-300236

Hess Michelini, R., A.L. Doedens, A.W. Goldrath, and S.M. Hedrick. 2013. Differentiation of CD8 memory T cells depends on Foxo1. *J. Exp. Med.* 210:1189–1200. http://dx.doi.org/10.1084/jem.20130392

Higashi, Y., M. Maruhashi, L. Nelles, T. Van de Putte, K. Verschueren, T. Miyoshi, A. Yoshimoto, H. Kondoh, and D. Huylebroeck. 2002. Generation of the floxed allele of the SIP1 (Smad-interacting protein 1) gene for Cre-mediated conditional knockout in the mouse. *Genesis.* 32:82–84. http://dx.doi.org/10.1002/gene.10048

Huster, K.M., V. Busch, M. Schiemann, K. Linkemann, K.M. Kerksiek, H. Wagner, and D.H. Busch. 2004. Selective expression of IL-7 receptor on memory T cells identifies early CD40L-dependent generation of distinct CD8⁺ memory T cell subsets. *Proc. Natl. Acad. Sci. USA.* 101:5610–5615. http://dx.doi.org/10.1073/pnas.0308054101

Ichii, H., A. Sakamoto, M. Hatano, S. Okada, H. Toyama, S. Taki, M. Arima, Y. Kuroda, and T. Tokuhisa. 2002. Role for Bcl-6 in the generation and maintenance of memory CD8⁺ T cells. *Nat. Immunol.* 3:558–563. http://dx.doi.org/10.1038/ni802

Ichii, H., A. Sakamoto, Y. Kuroda, and T. Tokuhisa. 2004. Bcl6 acts as an amplifier for the generation and proliferative capacity of central memory CD8⁺ T cells. *J. Immunol.* 173:883–891. http://dx.doi.org/10.4049/jimmunol.173.2.883

Jabbari, A., and J.T. Harty. 2006. Secondary memory CD8⁺ T cells are more protective but slower to acquire a central-memory phenotype. *J. Exp. Med.* 203:919–932. http://dx.doi.org/10.1084/jem.20052237

Jacob, J., and D. Baltimore. 1999. Modelling T-cell memory by genetic marking of memory T cells in vivo. *Nature.* 399:593–597. http://dx.doi.org/10.1038/21208

Jameson, S.C., and D. Masopust. 2009. Diversity in T cell memory: an embarrassment of riches. *Immunity.* 31:859–871. http://dx.doi.org/10.1016/j.immuni.2009.11.007

Jeannet, G., C. Boudousquié, N. Gardiol, J. Kang, J. Huelsken, and W. Held. 2010. Essential role of the Wnt pathway effector Tcf-1 for the establishment of functional CD8 T cell memory. *Proc. Natl. Acad. Sci. USA.* 107:9777–9782. http://dx.doi.org/10.1073/pnas.0914127107

Joshi, N.S., W. Cui, A. Chandele, H.K. Lee, D.R. Urso, J. Hagman, L. Gapin, and S.M. Kaech. 2007. Inflammation directs memory precursor and short-lived effector CD8⁺ T cell fates via the graded expression of T-bet

2054

ZEB2 programs terminal differentiation of CD8⁺ T cells | Dominguez et al.

transcription factor. *Immunity*. 27:281–295. http://dx.doi.org/10.1016/j .immuni.2007.07.010

Joshi, N.S., W. Cui, C.X. Dominguez, J.H. Chen, T.W. Hand, and S.M. Kaech. 2011. Increased numbers of preexisting memory CD8 T cells and decreased T-bet expression can restrain terminal differentiation of secondary effector and memory CD8 T cells. *J. Immunol*. 187:4068–4076. http://dx.doi.org/10.4049/jimmunol.1002145

Kaech, S.M., and W. Cui. 2012. Transcriptional control of effector and memory CD8+ T cell differentiation. *Nat. Rev. Immunol*. 12:749–761. http://dx.doi.org/10.1038/nri3307

Kaech, S.M., J.T. Tan, E.J. Wherry, B.T. Konieczny, C.D. Surh, and R. Ahmed. 2003. Selective expression of the interleukin 7 receptor identifies effector CD8 T cells that give rise to long-lived memory cells. *Nat. Immunol*. 4:1191–1198. http://dx.doi.org/10.1038/ni1009

Kallies, A., A. Xin, G.T. Belz, and S.L. Nutt. 2009. Blimp-1 transcription factor is required for the differentiation of effector CD8+ T cells and memory responses. *Immunity*. 31:283–295. http://dx.doi.org/10.1016/j .immuni.2009.06.021

Kim, K.O., E.R. Sampson, R.D. Maynard, R.J. O'Keefe, D. Chen, H. Drissi, R.N. Rosier, M.J. Hilton, and M.J. Zuscik. 2012. Ski inhibits TGF-β/ phospho-Smad3 signaling and accelerates hypertrophic differentiation in chondrocytes. *J. Cell. Biochem*. 113:2156–2166. http://dx.doi.org/10 .1002/jcb.24089

Kim, M.V., W. Ouyang, W. Liao, M.Q. Zhang, and M.O. Li. 2013. The transcription factor Foxo1 controls central-memory CD8+ T cell responses to infection. *Immunity*. 39:286–297. http://dx.doi.org/10 .1016/j.immuni.2013.07.013

Lazarevic, V., X. Chen, J.-H. Shim, E.-S. Hwang, E. Jang, A.N. Bolm, M. Oukka, V.K. Kuchroo, and L.H. Glimcher. 2011. T-bet represses T(H)17 differentiation by preventing Runx1-mediated activation of the gene encoding RORγt. *Nat. Immunol*. 12:96–104. http://dx.doi.org/10.1038 /ni.1969

Mackay, L.K., A. Rahimpour, J.Z. Ma, N. Collins, A.T. Stock, M.-L. Hafon, J. Vega-Ramos, P. Lauzurica, S.N. Mueller, T. Stefanovic, et al.. 2013. The developmental pathway for CD103+CD8+ tissue-resident memory T cells of skin. *Nat. Immunol*. 14:1294–1301. http://dx.doi.org/10.1038 /ni.2744

Masopust, D., V. Vezys, E.J. Wherry, D.L. Barber, and R. Ahmed. 2006. Cutting edge: gut microenvironment promotes differentiation of a unique memory CD8 T cell population. *J. Immunol*. 176:2079–2083. http://dx .doi.org/10.4049/jimmunol.176.4.2079

Mathelier, A., X. Zhao, A.W. Zhang, F. Parcy, R. Worsley-Hunt, D.J. Arenillas, S. Buchman, C.Y. Chen, A. Chou, H. Ienasecu, et al.. 2014. JASPAR 2014: an extensively expanded and updated open-access database of transcription factor binding profiles. *Nucleic Acids Res*. 42:D142–D147. http://dx.doi.org/10.1093/nar/gkt997

Mollo, S.B., J.T. Ingram, R.L. Kress, A.J. Zajac, and L.E. Harrington. 2013. Virus-specific CD4 and CD8 T cell responses in the absence of Th1-associated transcription factors. *J. Leukoc. Biol*.

Nam, E.-H., Y. Lee, Y.-K. Park, J.W. Lee, and S. Kim. 2012. ZEB2 upregulates integrin α5 expression through cooperation with Sp1 to induce invasion during epithelial-mesenchymal transition of human cancer cells. *Carcinogenesis*. 33:563–571. http://dx.doi.org/10.1093/carcin/bgs005

Oestreich, K.J., A.C. Huang, and A.S. Weinmann. 2011. The lineage-defining factors T-bet and Bcl-6 collaborate to regulate Th1 gene expression patterns. *J. Exp. Med*. 208:1001–1013. http://dx.doi.org/10.1084/jem .20102144

Olson, J.A., C. McDonald-Hyman, S.C. Jameson, and S.E. Hamilton. 2013. Effector-like CD8+ T cells in the memory population mediate potent protective immunity. *Immunity*. 38:1250–1260. http://dx.doi.org/10 .1016/j.immuni.2013.05.009

Omilusik, K.D., J. Adam Best, B. Yu, S. Goossens, A. Weidemann, J.V. Nguyen, E. Seuntjens, A. Stryjewska, C. Zweier, R. Roychoudhuri, et al.. 2015. Transcriptional repressor ZEB2 promotes terminal differentiation of CD8+ effector and memory T cell populations during infection. *J. Exp. Med*. http://dx.doi.org/10.1084/jem.20090525

Rutishauser, R.L., and S.M. Kaech. 2010. Generating diversity: transcriptional regulation of effector and memory CD8 T-cell differentiation. *Immunol. Rev*. 235:219–233.

Rutishauser, R.L., G.A. Martins, S. Kalachikov, A. Chandele, I.A. Parish, E. Meffre, J. Jacob, K. Calame, and S.M. Kaech. 2009. Transcriptional repressor Blimp-1 promotes CD8+ T cell terminal differentiation and represses the acquisition of central memory T cell properties. *Immunity*. 31:296–308. http://dx.doi.org/10.1016/j.immuni.2009.05.014

Sallusto, F., D. Lenig, R. Förster, M. Lipp, and A. Lanzavecchia. 1999. Two subsets of memory T lymphocytes with distinct homing potentials and effector functions. *Nature*. 401:708–712. http://dx.doi.org/10.1038 /44385

Sánchez Alvarado, A., and S. Yamanaka. 2014. Rethinking differentiation: stem cells, regeneration, and plasticity. *Cell*. 157:110–119. http://dx.doi .org/10.1016/j.cell.2014.02.041

Schluns, K.S., W.C. Kieper, S.C. Jameson, and L. Lefrançois. 2000. Interleukin-7 mediates the homeostasis of naïve and memory CD8 T cells in vivo. *Nat. Immunol*. 1:426–432. http://dx.doi.org/10.1038/80868

Shin, H.M., V.N. Kapoor, T. Guan, S.M. Kaech, R.M. Welsh, and L.J. Berg. 2013. Epigenetic modifications induced by Blimp-1 regulate CD8+ T cell memory progression during acute virus infection. *Immunity*. 39:661–675. http://dx.doi.org/10.1016/j.immuni.2013.08.032

Takemoto, N., A.M. Intlekofer, J.T. Northrup, E.J. Wherry, and S.L. Reiner. 2006. Cutting Edge: IL-12 inversely regulates T-bet and eomesodermin expression during pathogen-induced CD8+ T cell differentiation. *J. Immunol*. 177:7515–7519. http://dx.doi.org/10.4049/jimmunol.177.11 .7515

Tejera, M.M., E.H. Kim, J.A. Sullivan, E.H. Plisch, and M. Suresh. 2013. FoxO1 controls effector-to-memory transition and maintenance of functional CD8 T cell memory. *J. Immunol*. 191:187–199. http://dx.doi .org/10.4049/jimmunol.1300331

Teo, A.K., S.J. Arnold, M.W. Trotter, S. Brown, L.T. Ang, Z. Chng, E.J. Robertson, N.R. Dunn, and L. Vallier. 2011. Pluripotency factors regulate definitive endoderm specification through eomesodermin. *Genes Dev*. 25:238–250. http://dx.doi.org/10.1101/gad.607311

Thimme, R., V. Appay, M. Koschella, E. Panther, E. Roth, A.D. Hislop, A.B. Rickinson, S.L. Rowland-Jones, H.E. Blum, and H. Pircher. 2005. Increased expression of the NK cell receptor KLRG1 by virus-specific CD8 T cells during persistent antigen stimulation. *J. Virol*. 79:12112–12116. http://dx.doi.org/10.1128/JVI.79.18.12112-12116.2005

Tse, S.-W., I.A. Cockburn, H. Zhang, A.L. Scott, and F. Zavala. 2013. Unique transcriptional profile of liver-resident memory CD8+ T cells induced by immunization with malaria sporozoites. *Genes Immun*. 14:302–309. http ://dx.doi.org/10.1038/gene.2013.20

Tylzanowski, P., D. De Valck, V. Maes, J. Peeters, and F.P. Luyten. 2003. Zfhx1a and Zfhx1b mRNAs have non-overlapping expression domains during chick and mouse midgestation limb development. *Gene Expr. Patterns*. 3:39–42. http://dx.doi.org/10.1016/S1567-133X(02)00092-3

van Grunsven, L.A., V. Taelman, C. Michiels, K. Opdecamp, D. Huylebroeck, and E.J. Bellefroid. 2006. deltaEF1 and SIP1 are differentially expressed and have overlapping activities during *Xenopus* embryogenesis. *Dev. Dyn*. 235:1491–1500. http://dx.doi.org/10.1002/dvdy.20727

Verstappen, G., L.A. van Grunsven, C. Michiels, T. Van de Putte, J. Souopgui, J. Van Damme, E. Bellefroid, J. Vandekerckhove, and D. Huylebroeck. 2008. Atypical Mowat-Wilson patient confirms the importance of the novel association between ZFHX1B/SIP1 and NuRD corepressor complex. *Hum. Mol. Genet*. 17:1175–1183. http://dx.doi.org/10.1093/hmg/ ddn007

Voehringer, D., C. Blaser, P. Brawand, D.H. Raulet, T. Hanke, and H. Pircher. 2001. Viral infections induce abundant numbers of senescent CD8 T cells. *J. Immunol.* 167:4838–4843. http://dx.doi.org/10.4049/jimmunol.167.9.4838

Wakim, L.M., A. Woodward-Davis, R. Liu, Y. Hu, J. Villadangos, G. Smyth, and M.J. Bevan. 2012. The molecular signature of tissue resident memory CD8 T cells isolated from the brain. *J. Immunol.* 189:3462–3471. http://dx.doi.org/10.4049/jimmunol.1201305

Wang, J., S. Lee, C.E.-Y. Teh, K. Bunting, L. Ma, and M.F. Shannon. 2009. The transcription repressor, ZEB1, cooperates with CtBP2 and HDAC1 to suppress IL-2 gene activation in T cells. *Int. Immunol.* 21:227–235. http://dx.doi.org/10.1093/intimm/dxn143

Wherry, E.J., J.N. Blattman, K. Murali-Krishna, R. van der Most, and R. Ahmed. 2003a. Viral persistence alters CD8 T-cell immunodominance and tissue distribution and results in distinct stages of functional impairment. *J. Virol.* 77:4911–4927. http://dx.doi.org/10.1128/JVI.77.8.4911-4927.2003

Wherry, E.J., V. Teichgräber, T.C. Becker, D. Masopust, S.M. Kaech, R. Antia, U.H. von Andrian, and R. Ahmed. 2003b. Lineage relationship and protective immunity of memory CD8 T cell subsets. *Nat. Immunol.* 4:225–234. http://dx.doi.org/10.1038/ni889

Wirth, T.C., H.-H. Xue, D. Rai, J.T. Sabel, T. Bair, J.T. Harty, and V.P. Badovinac. 2010. Repetitive antigen stimulation induces stepwise transcriptome diversification but preserves a core signature of memory CD8^{+} T cell differentiation. *Immunity.* 33:128–140. http://dx.doi.org/10.1016/j.immuni.2010.06.014

Yang, C.Y., J.A. Best, J. Knell, E. Yang, A.D. Sheridan, A.K. Jesionek, H.S. Li, R.R. Rivera, K.C. Lind, L.M. D'Cruz, et al.. 2011. The transcriptional regulators Id2 and Id3 control the formation of distinct memory CD8^{+} T cell subsets. *Nat. Immunol.* 12:1221–1229. http://dx.doi.org/10.1038/ni.2158

Zhou, X., S. Yu, D.-M. Zhao, J.T. Harty, V.P. Badovinac, and H.-H. Xue. 2010. Differentiation and persistence of memory CD8^{+} T cells depend on T cell factor 1. *Immunity.* 33:229–240. http://dx.doi.org/10.1016/j.immuni.2010.08.002

ZEB2 programs terminal differentiation of CD8^{+} T cells | Dominguez et al.